Received: 19 December 2017 | Revised: 16 January 2018 | Accepted: 24 January 2018

DOI: 10.1002/hbm.23992

RESEARCH ARTICLE

WILEY

Multiscale energy reallocation during low-frequency steady-state brain response

Yifeng Wang[1,2] | Wang Chen[1,2] | Liangkai Ye[1,2] | Bharat B. Biswal[1,2,4] | Xuezhi Yang[1,2] | Qijun Zou[1,2] | Pu Yang[1,2] | Qi Yang[1,2] | Xinqi Wang[1,2] | Qian Cui[1,3] | Xujun Duan[1,2] | Wei Liao[1,2] | Huafu Chen[1,2]

[1]The Clinical Hospital of Chengdu Brain Science Institute, MOE Key Lab for Neuroinformation, University of Electronic Science and Technology of China, Chengdu 611731, China

[2]School of Life Science and Technology, Center for Information in BioMedicine, University of Electronic Science and Technology of China, Chengdu 611731, China

[3]School of Political Science and Public Administration, University of Electronic Science and Technology of China, Chengdu 611731, China

[4]Department of Biomedical Engineering, New Jersey Institute of Technology, 607 Fenster Hall, University Height, Newark, New Jersey 07102

Correspondence
Huafu Chen, The Clinical Hospital of Chengdu Brain Science Institute, MOE Key Lab for Neuroinformation, University of Electronic Science and Technology of China, Chengdu 611731, China.
Email: chenhf@uestc.edu.cn Or Yifeng Wang, The Clinical Hospital of Chengdu Brain Science Institute, MOE Key Lab for Neuroinformation, University of Electronic Science and Technology of China, Chengdu 611731, China.
Email: wangyif@uestc.edu.cn

Funding information
863 Project, Grant/Award Number: 2015AA020505; 111 project, Grant/Award Number: B12027; Natural Science Foundation of China, Grant/Award Numbers: 61533006, 31600930, 31400901, 61673089; Science Foundation of Ministry of Education of China, Grant/Award Number: 14XJC190003; Fundamental Research Funds for the Central Universities, Grant/Award Numbers: ZYGX2016KYQD120, ZYGX2015J141

Abstract

Traditional task-evoked brain activations are based on detection and estimation of signal change from the mean signal. By contrast, the low-frequency steady-state brain response (lfSSBR) reflects frequency-tagging activity at the fundamental frequency of the task presentation and its harmonics. Compared to the activity at these resonant frequencies, brain responses at nonresonant frequencies are largely unknown. Additionally, because the lfSSBR is defined by power change, we hypothesize using Parseval's theorem that the power change reflects brain signal variability rather than the change of mean signal. Using a face recognition task, we observed power increase at the fundamental frequency (0.05 Hz) and two harmonics (0.1 and 0.15 Hz) and power decrease within the infra-slow frequency band (<0.1 Hz), suggesting a multifrequency energy reallocation. The consistency of power and variability was demonstrated by the high correlation ($r > .955$) of their spatial distribution and brain–behavior relationship at all frequency bands. Additionally, the reallocation of finite energy was observed across various brain regions and frequency bands, forming a particular spatiotemporal pattern. Overall, results from this study strongly suggest that frequency-specific power and variability may measure the same underlying brain activity and that these results may shed light on different mechanisms between lfSSBR and brain activation, and spatiotemporal characteristics of energy reallocation induced by cognitive tasks.

KEYWORDS
brain signal variability, face recognition, fMRI, frequency specificity, steady-state brain response

1 | INTRODUCTION

Low-frequency steady-state brain response (lfSSBR) refers to enhanced power of brain signal at the fundamental frequency of cognitive task and its harmonics (Herrmann, 2001; Wang et al., 2014). This is different from traditional brain analysis, where activation measured by the general linear model (GLM). In lfSSBR, we assess the amplitude of regular fluctuations in a relative long time series rather than transient signal change (Figure 1), indicating that it cannot be delineated using traditional hemodynamic response function (Lewis, Setsompop, Rosen, & Polimeni, 2016; Wang et al., 2014). Additionally, the lfSSBR represents brain network in frequency- and phase-dependent means (Wang, Liu,

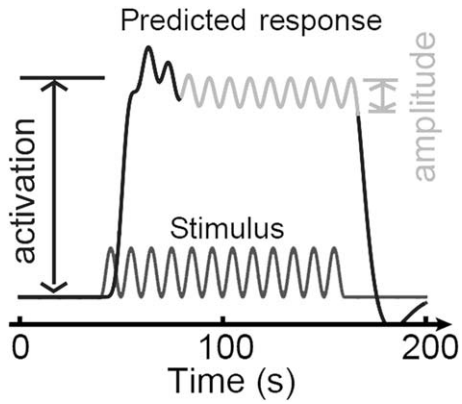

FIGURE 1 The schematic plot of activation and lfSSBR. Brain activation measures the transient enhancement of brain signal, whereas the lfSSBR surveys the amplitude of signal fluctuations in a relative long term

Jing, Long, & Chen, 2016a; Wang et al., 2016b), and is associated with particular psychophysiological activity (Wang et al., 2014, 2015). Recent studies have suggested that task-evoked blood oxygen level dependent (BOLD) signals and ongoing BOLD signal fluctuations have negative and phase-dependent interaction, challenging the linear superposition model (He, 2013; Huang et al., 2017). It has also been suggested that stochastic fluctuations are physiologically meaningful rather than pure noise, and therefore, should not be simply eliminated by averaging across trials (Garrett, Kovacevic, McIntosh, & Grady, 2010; McDonnell & Ward, 2011). These findings indicate that lfSSBR can serve as an alternative index of brain activity, though its exact neural mechanism is not completely understood.

The power of signal in the frequency domain is equivalent to the variability in the time domain and vice versa based on the Parseval's theorem. Accordingly, we hypothesize that the lfSSBR may reflect brain signal variability (BSV) at particular frequencies. Previous studies have shown enhanced power, functional connectivity, and coherence at resonant frequencies (the fundamental frequency and its harmonics) and a reduction in power at lower frequency range (Fransson, 2006; He, 2011; Wang et al., 2014, 2015), suggesting frequency-specific characteristics of lfSSBR. The BSV, on the other hand, is usually measured at broad frequency range (Garrett et al., 2013b; Guitart-Masip et al., 2016), leaving its frequency characteristics largely unknown. Therefore, systematically investigating the frequency characteristics of power and variability would help understand the lfSSBR mechanism.

The primary aim of the article is to explore the mechanism of lfSSBR by comparing it with BSV at multiple frequency bands through two steps: (a) inspecting the spatial distribution of task effect on power and variability and (b) investigating behavioral correlation of power and variability. Results from this study suggest high consistency between these two indices and significant frequency specificity for both of them. These evidence demonstrate that the lfSSBR in the frequency domain reflects BSV in the time domain, improving our understanding of the time–frequency mechanism of lfSSBR.

2 | METHODS

2.1 | Subjects and procedure

Thirty participants (mean age ± standard deviation (*SD*) = 22.41 ± 2.11 years, range from 18 to 27 years; 15 males/15 females) were recruited for this study. All the subjects had normal or correct-to-normal vision, were right-handed, reported free from any medication, neurological, and psychiatric disorders. Written informed consent, approved by the research ethical committee of School of Life Science and Technology at University of Electronic Science and Technology of China, was obtained from each subject before the beginning of the experiment. The experiment was carried out in accordance with The Code of Ethics of the World Medical Association (Declaration of Helsinki).

A task lasting for 10 min 20 s and an equal-length resting scan were counterbalanced between subjects. During the task presentations, participants were asked to perform a face recognition task by judging whether the face has a neutral expression (right thumb response) or happy expression (left thumb response) as accurately and fast as possible. Although there were only neutral faces in the paradigm, subjects were told that happy expression appeared no more than once to ensure that they paid attention during the entire task. The stimuli were selected from the Chinese Facial Affective Picture System (CFAPS). The values of valence, arousal, dominance, and attraction were 4.40 ± 0.60 (mean ± *SD*), 3.65 ± 0.54, 4.98 ± 0.35, and 4.19 ± 0.45, respectively. In each trial, the face was presented on the black background for 2 s and followed by a white fixation crosshair of 18 s. Each trial lasted for 20 s, forming a fundamental frequency of 0.05 Hz. The procedure was performed with E-Prime 2.0 software (http://www.pstnet.com; Psychology Software Tools). During the resting scan, participants were required to remain motionless, focus their eyes on a white crosshair against black background, stay awake, and not think of anything in particular.

2.2 | Imaging data acquisition

MRI data were acquired using a 3.0 T GE 750 scanner (General Electric, Fairfield, Connecticut, USA) equipped with high-speed gradients. An 8-channel prototype quadrature birdcage head coil fitted with foam padding was applied to minimize the head motion. Functional images were acquired using a gradient-recalled echo-planar imaging (EPI) sequence. The imaging parameters were as follows: repetition time/echo time = 2,000 ms/30 ms, 90° flip angle, bandwidth = 250 Hz/pixel, 43 axial slices (3.2 mm slice thickness without gap), 64 × 64 matrix, 22 cm field of view, and 310 volumes.

2.3 | Imaging data preprocessing

Functional images were preprocessed using the Data Processing Assistant for Resting-state fMRI (DPARSF 2.3, http://www.restfmri.net/forum/DPARSF). The preprocessing flow was determined by previous variability and lfSSBR studies and is therefore briefly described here (Garrett, Kovacevic, McIntosh, & Grady, 2013a; Garrett, McIntosh, & Grady, 2014; Wang et al., 2014, 2015). The first 10 volumes were

discarded to ensure signal equilibrium and for the participants to familiarize themselves with the scanning environment (Wang et al., 2014). The remaining 300 images were slice-time corrected, spatially aligned, spatially normalized to Montreal Neurological Institute (MNI) EPI template, and resampled to $3 \times 3 \times 3$ voxels. The images were then spatially smoothed with 8-mm FWHM Gaussian kernel. Friston's 24 head motion parameters, white matter signal and cerebrospinal fluid signal were further regressed out using DPARSF. The data of one participant were removed from the final analysis due to large head motion (translation >3 mm or rotation $>3°$) in any scan.

2.4 | Behavioral data analysis

The accuracy and reaction time (RT) of behavioral performance were calculated for each subject.

2.5 | Whole-brain power analysis

Whole-brain power analysis was first performed to determine whether lfSSBR was evoked by the task and to define the boundary of each frequency band. This analysis has been depicted elsewhere in detail (Wang et al., 2014), and therefore, only briefly described here. We first defined the gray matter region within the Automated Anatomical Labeling (AAL) 90 template. The time series of each voxel in the gray matter was converted to the frequency domain without band-pass filtering using the fast Fourier transform (FFT). The frequency resolution is 0.0017 Hz (sampling rate/data length: 0.5 Hz/300). The power spectrum of task state or resting state for each subject was defined as the average of power spectrum in all voxels. The frequency-specific mean power was calculated at all resonant (0.0475–0.0525 Hz (the fundamental frequency), 0.0975–0.1025 Hz (the first harmonic), 0.1475–0.1525 Hz (the second harmonic), 0.1975–0.2025 Hz (the third harmonic)), and nonresonant (0.01–0.0475 Hz, 0.0525–0.0975 Hz, 0.1025–0.1475 Hz, 0.1525–0.1975 Hz, 0.2025–0.25 Hz) frequency bands. Paired-samples t test was used to assess in which frequency band the power was modulated by task. Multiple comparisons were corrected by Bonferroni approach with $p < .05$ (Wang et al., 2013).

2.6 | Regional power analysis

Preprocessed data were band-pass filtered into aforementioned nine frequency bands using the DPARSF software. The power was calculated in each voxel of the gray matter mask within these frequency bands. The obtained power values were transformed to standard z values to reduce the global effects of variance across participants (Yan & Zang, 2010) and enable the comparison between two indices (Liang, Zou, He, & Yang, 2013). For each subject, the z value of each voxel was obtained by subtracting the mean and dividing by the standard deviation of all voxels. Paired-samples t test was performed in each frequency band to evaluate the task effect. All resulting maps were corrected using false discovery rate (FDR) method ($p < .05$) for multiple comparisons (Worsley et al., 1996). Statistical analyses were conducted with SPM8 (www.fil.ion.ucl.ac.uk/spm). Considering the rigidity of correction for multiple comparisons, we also computed the group level z maps of power as well as the ratio of z value of task/rest at each frequency band to show the spatial pattern of power.

It should be noticed that percent-signal change or z-statistics of time series are often used in BSV studies because the MSSD is sensitive to field-strength; however, the normalization of time series is not often used in lfSSBR or power studies (Guitart-Masip et al., 2016; Nomi, Bolt, Ezie, Uddin, & Heller, 2017; Samanez-Larkin, Kuhnen, Yoo, & Knutson, 2010; Wang et al., 2016b; Yang et al., 2007). In addition, Nomi et al. (2017) compared the MSSD with normalized time series and SD with non-normalized time series, observing a correlation of 0.73 between two indices. By contrast, Garrett, Kovacevic, McIntosh, and Grady (2011) reported strongly correlated ($r > .97$) MSSD and SD using normalized time series. It seems that the normalization of time series may induce dramatic change of BSV. Here, we calculated the power at the fundamental frequency from time series before and after z transformation. The power map with normalized time series is largely different from the power map with raw time series (Figure 2). Of note, some important brain regions for face recognition such as the occipital face area and fusiform face area are drowned in other regions when using normalized time series. In fact, cognitive tasks can evoke high power or amplitude in particular regions (Rossion, Prieto, Boremanse, Kuefner, & Van Belle, 2012; Wang et al., 2014). The inter-regional difference in response strength is of importance for the location of task effect. Although normalized data could reflect different response strengths of one region to distinctive tasks or brain states, it could also change the relative response strengths of different brain regions. To better describe task-related functional organization of the brain, we decided to use non-normalized time series in both power and BSV analyses.

2.7 | Moment-to-moment signal variability

The mean squared successive difference (MSSD) was adopted to represent temporal variability of both task and resting states. MSSD is considered as an appropriate metric of temporal variability in experiments with different cognitive situations (Mohr & Nagel, 2010; Samanez-Larkin et al., 2010). For each voxel in the gray matter, the MSSD was computed by subtracting a time point from the next time point, squaring the difference, then averaging all values over the whole time series. The calculation was accomplished with a custom-built function in MATLAB (The MathWorks, Inc.) within the same nine frequency bands as regional power analysis based on band-pass filtered data. The variability effect was tested using the same statistical approach as the regional power (see the previous paragraph).

2.8 | Cross-frequency coupling

We adopted the cross-voxel correlation (CVC) (Liang et al., 2013) to evaluate the similarity of spatial distribution between power and variability. As suggested by Liang et al., the 3D z maps of lfSSBR and variability within the gray matter were first transformed into columns,

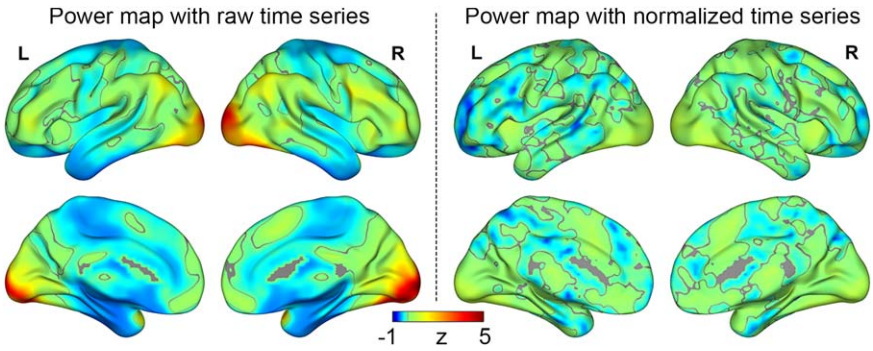

FIGURE 2 Power distributions obtained from data without (left) and with (right) *z* transformation at the fundamental frequency. The two distribution patterns are different from each other with spatial correlation coefficient $r = 0.4455$. The face recognition regions (e.g., the occipital face area and fusiform face area) cannot be differentiated from other regions using data after *z* transformation [Color figure can be viewed at wileyonlinelibrary.com]

respectively. The gray matter mask was used to ensure cross-frequency comparison in the same region and to test whether power and variability reflect the same response pattern in both task and nontask regions because various patterns of response could be detected in the whole brain with high signal-to-noise ratio (SNR) (Gonzalez-Castillo et al., 2012). The Pearson's correlation was computed between two columns of data. To estimate the *p* values, the effective degree of freedom (df_{eff}) in the CVC analysis was corrected, considering the dependence between voxels influenced by spatial smoothing (Liang et al., 2013). The intra- and interfrequency correlations of power–power, variability–variability, and power–variability were calculated for both task and resting states. The differences in these correlations between task and resting states and between adjacent frequency bands were measured by paired-samples *t* test. The results of *t* test were corrected for multiple comparisons using FDR approach ($p < .05$).

2.9 | Brain–behavior relationship

Because the BSV measures the variance of time series rather than mean BOLD signal (Garrett et al., 2010) and is thought to be associated with behavioral stability (McIntosh, Kovacevic, & Itier, 2008), we assessed the correlations between the power and variability of task state and the mean and SD of RT at all frequency bands. Here, *r* values over ±0.7 were categorized as strong correlations, *r* values over ±0.4 were interpreted as moderate correlations, and those over ±0.1 were weak correlations (Sokunbi, 2014). The CVC of correlation maps was further performed to assess the similarity of intra- and interfrequency spatial distribution of brain–behavior relationship.

TABLE 1 Task-induced power increase or decrease at multiple frequency bands

Frequency band	$t_{(28)}$	p^a	Cohen's *d*
Fundamental	6.427	<.0001	1.404
First harmonic	4.386	.0001	1.170
Second harmonic	5.367	<.0001	1.283
0.01–0.0475 Hz	−3.890	.0006	0.780

[a]Paired-samples *t* test with Bonferroni correction, $p < .05$.

3 | RESULTS

3.1 | Behavioral results

The accuracy of performance was extremely high with only two incorrect responses out of 870 trials in all 29 subjects. At the group level, the RT was 624.67 ± 107.47 (mean ± *SD*) ms. It ranged from 344.32 to 875.43 ms at the individual level with the *SD* ranging from 50.88 to 184.80 ms.

3.2 | Frequency-specific power reallocation at the whole-brain level

Compared to resting state, the power was increased at the fundamental frequency of task, the first and second harmonics while decreased

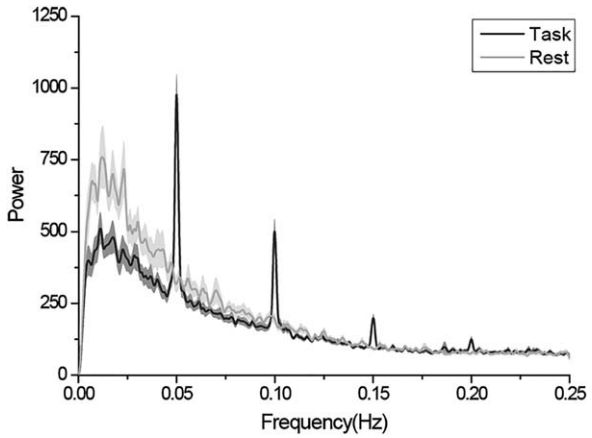

FIGURE 3 Whole brain power spectrums in task and resting states. Compared with resting state, the face recognition task enhanced the power at the fundamental frequency of task and two harmonics, showing evident lfSSBR. Besides that, the task reduced the power in the lower frequency band. Solid lines show the mean values of power for all subjects. Shaded areas are defined by standard error

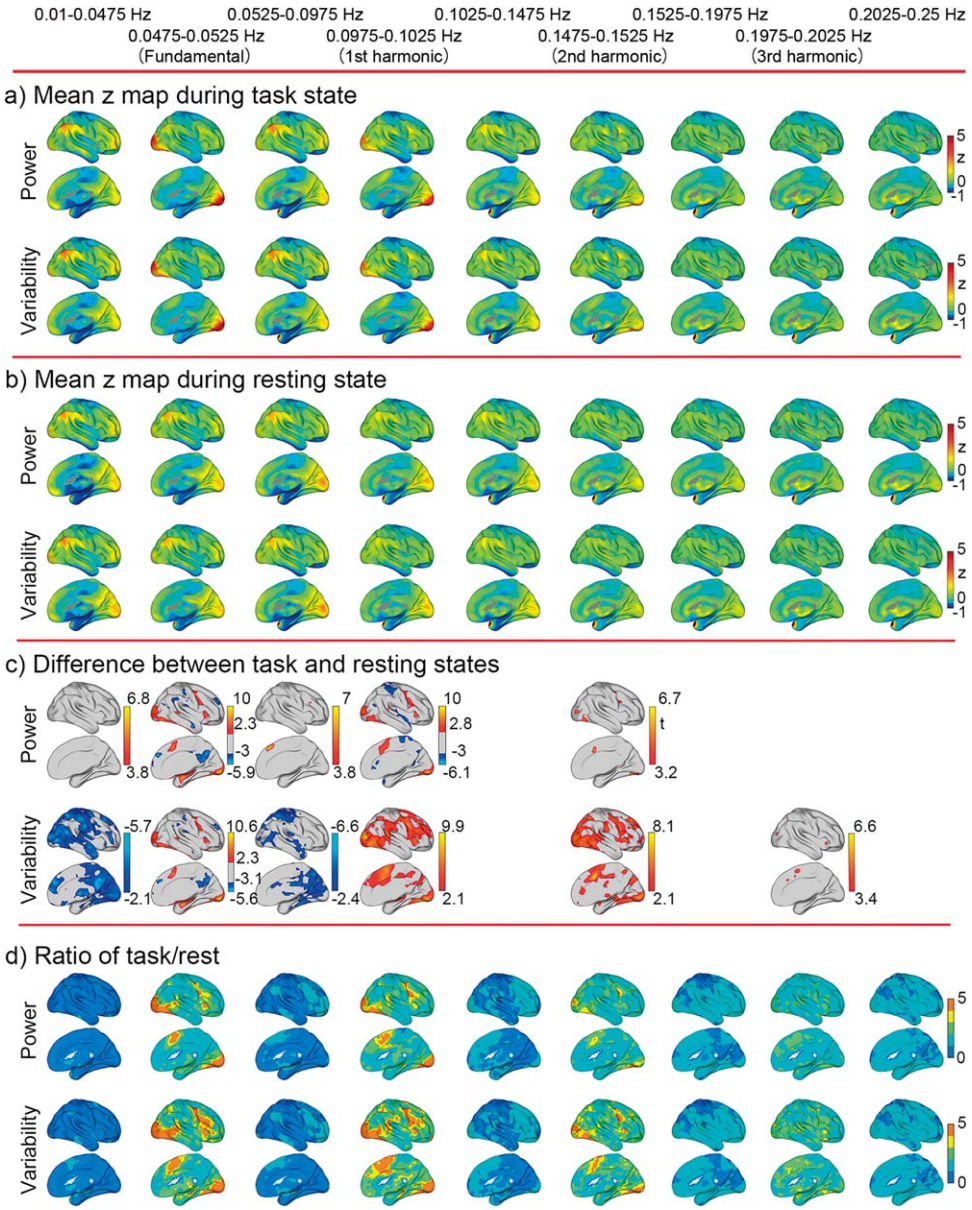

FIGURE 4 The spatial distribution of power and variability and their task effects within nine frequency bands. The group level spatial distribution of power and variability is obtained by averaging the z map of each subject (a,b). The task effect is revealed by paired-samples *t* test (c). To eliminate the restriction of stringent multiple comparison correction, the ratio of z value of task/rest is shown by averaging the ratio of each subject (d). Only the right hemisphere is shown [Color figure can be viewed at wileyonlinelibrary.com]

at the 0.01–0.0475 Hz frequency band (Table 1 and Figure 3), showing frequency-specific power reallocation.

3.3 | Frequency-specific spatial distribution of power and variability

In line with previous findings (Baria, Baliki, Parrish, & Apkarian, 2011; Zuo et al., 2010), the power transferred from the cortical regions to subcortical structures as frequency increases (Figure 4a,b). The variability showed the same trend as power. The task effects for both power and variability appeared at the fundamental frequency and its harmonics as well as two infra-slow frequency bands (0.01–0.0475 Hz, and 0.0525–0.0975 Hz). However, regions with task effect for power were similar to those for variability only at the fundamental frequency (Figure 4c). At the fundamental frequency, task evoked higher power and variability in the core regions of face recognition (occipital face area (OFA), fusiform face area (FFA), posterior superior temporal sulcus (pSTS)) (Haxby, Hoffman, & Gobbini, 2000), attention regions (anterior insula, inferior frontal junction) (Baldauf & Desimone, 2014), and motor region (supplementary motor area (SMA)) (Bonini et al., 2014) and decreased power and variability in the default mode network (posterior cingulate cortex (PCC)/precuneus, angular gyrus, medial, and lateral frontal cortex) (Raichle, 2015). The pattern of increased and decreased power/variability is similar to task-relevant brain activation and deactivation. Significantly increased power was found at 0.01–0.0475 and 0.0525–0.0975 Hz, whereas significantly decreased variability was

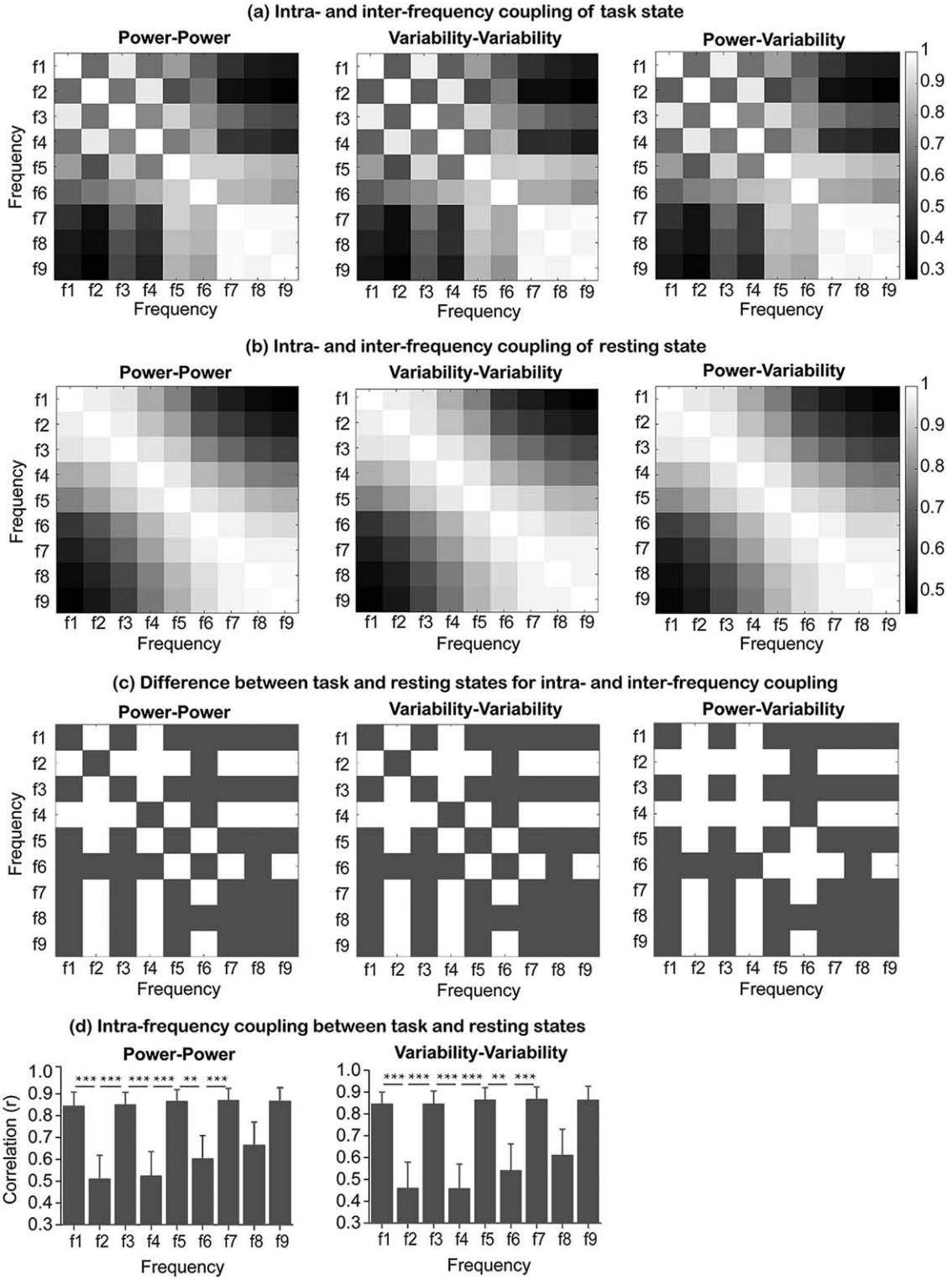

FIGURE 5 The intra- and interfrequency coupling for power and variability in task and resting states and their differences between these two states. The cross-voxel correlation is used to measure the spatial coupling in task (a) and resting (b) states. The difference between task and resting states is assessed by paired-samples *t* test and shown with white color (c). Intrafrequency coupling between task and resting states shows that spatial couplings are reduced at resonant frequencies compared with nonresonant frequencies (d). The task effect is also measured between adjacent frequency bands (d). Symbols f1–f9 correspond to nine frequency bands from 0.01–0.0475 Hz to 0.2025–0.25 Hz. Color bar indexes the *r* value in panel a and b. ** represents $p < .01$, while *** represents $p < .001$ in panel d

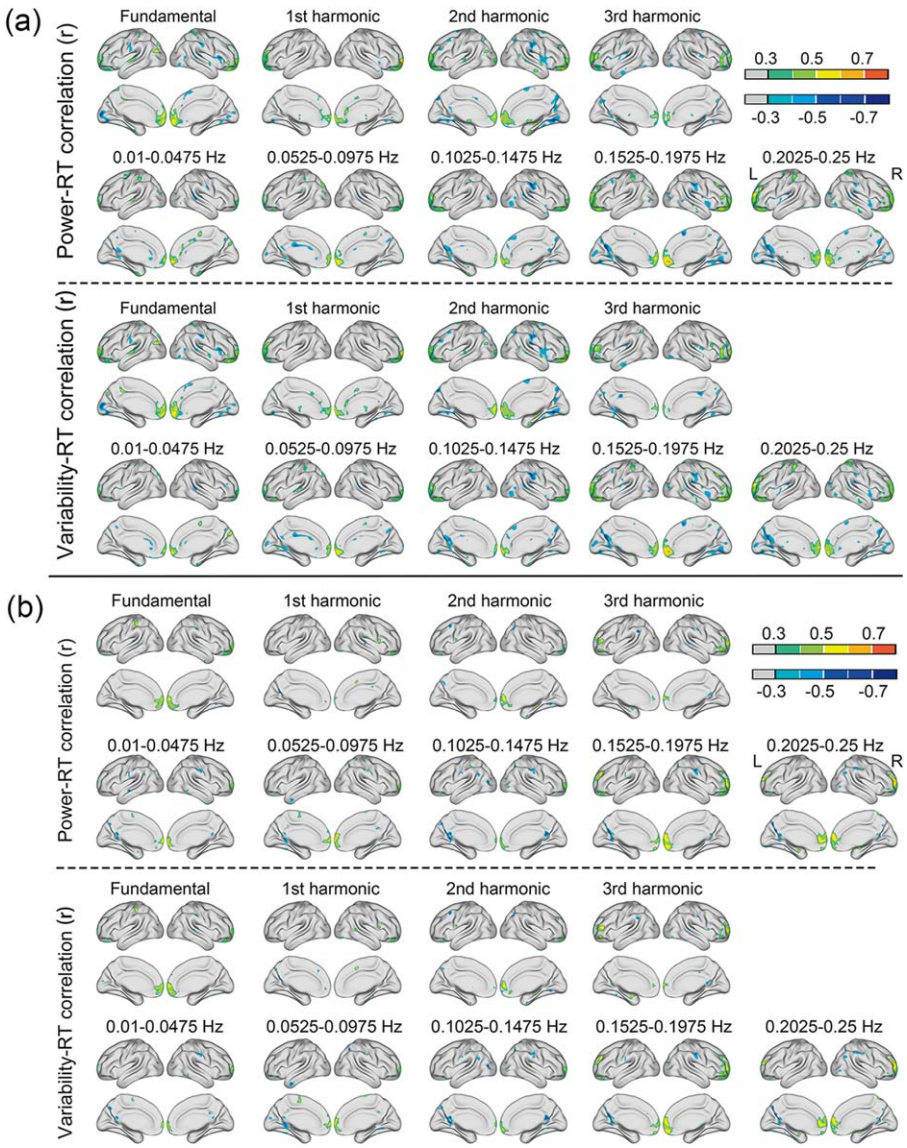

FIGURE 6 The brain–behavior correlation. Panel a shows the correlation coefficient maps between power/variability and the mean of RT. Panel b shows the correlation coefficient maps between power/variability and the SD of RT. Color bar shows the range of correlation coefficient [Color figure can be viewed at wileyonlinelibrary.com]

observed in these frequency bands. Only enhanced variability was observed at three harmonics, whereas reduced power was found at the first harmonic in the auditory and somatosensory regions (Figure 4c). However, these discrepant effects between power and variability might be due to different statistical validities because the task induced spatial patterns were much similar between power and variability.

3.4 | Consistent spatial distribution of power and variability

Besides the ratio map of task/rest, the CVC analysis further demonstrated that the spatial distributions of variability and power were highly consistent ($r > .993$) at the same frequency band for both task and resting states, indicating that power and variability reflect the same response pattern not only in task regions but also in nontask regions. The highly similar spatial pattern during rest and task states made the two distributions highly consistent in intra- and interfrequency coupling (Figure 5a,b). The task effect on spatial distribution showed frequency-specific characteristics between resonant and nonresonant frequency bands (Figure 5c) which might be caused by task-rest decoupling at resonant frequencies (Figure 5d).

3.5 | Brain–behavior relationship

After demonstrating reliable spatial distributions of power and variability, we further investigated whether the two indices have a consistent brain–behavior relationship. Strongly positive correlation was observed between power/variability and the mean of RT in the frontal pole, whereas strongly negative correlations were found in the face recognition regions (the primary visual cortex, FFA, and pSTS), the attention

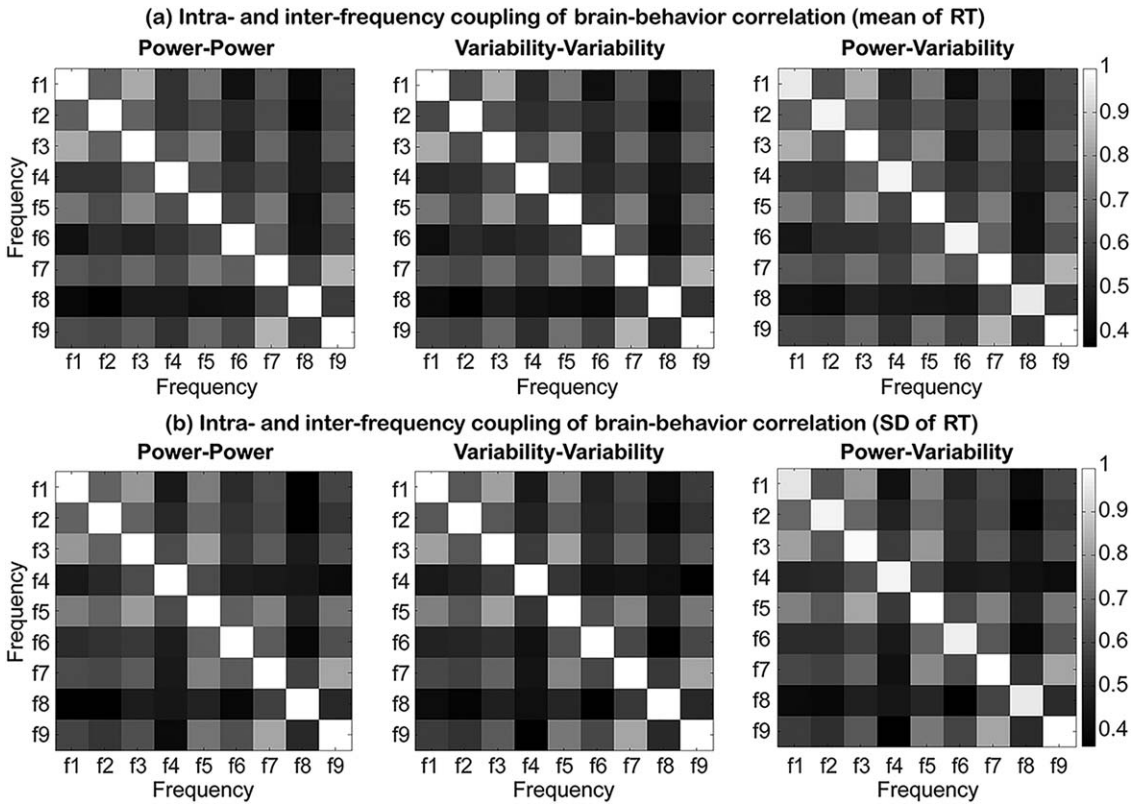

FIGURE 7 The intra- and interfrequency coupling of brain–behavior relationship. The cross-voxel correlation is used to measure the spatial coupling of brain–behavior correlation between power/variability and the mean of RT (a) and the SD of RT (b). Symbols f1–f9 correspond to nine frequency bands from 0.01–0.0475 Hz to 0.2025–0.25 Hz. Color bar indexes the *r* value

related areas (the anterior insula and precuneus), and sensorimotor regions (the SMA, middle cingulate cortex, and somatosensory cortex). A similar brain–behavior relationship was found between the SD of RT and power/variability (Figure 6). Of note, the brain–behavior relationship dispersed at both resonant and nonresonant frequency bands, indicating the multifrequency physiological meanings of power/variability.

3.6 | Consistent spatial distribution of brain–behavior relationship for power and variability

The spatial distributions of brain–behavior correlation for power and variability were highly consistent (CVC, $r > .955$) at the same frequency band (Figure 7). The intra- and interfrequency power-variability coupling mirrored the power–power and variability–variability couplings, confirming the high consistency of the brain–behavior relationship between power and variability.

4 | DISCUSSION

In this study, we explored the mechanism of lfSSBR, demonstrating the equivalence of power and variability in the corresponding frequency bands with powerful empirical evidence. Specifically, the lfSSBR, unlike brain activation, is associated with the variance of brain signal. This study further demonstrated reallocation of energy at multiple frequency bands during face recognition.

4.1 | The consistency of power in the frequency domain and variability in the time domain

Both spatial distribution and brain–behavior relationship show a high consistency of power and variability, suggesting the equivalence of power and variability in the corresponding frequency ranges. The lfSSBR and brain activation are associated with the variance and mean of brain signal (Lewis et al., 2016; also see Figure 1), demonstrating different mechanisms between them. Due to the high consistency between power and variability, we can comprehend both of them from perspectives of energy consumption, complex system, and frequency specificity.

The BSV is suggested to be associated with the dynamic range of brain function, or kinetic energy of the brain to achieve various potential states (Garrett et al., 2014), indicating that it reflects energy consumption within a period of time. Therefore, the consistency of power and variability guarantees the equivalence of energy consumption in the particular frequency band and that in corresponding temporal scale. Accordingly, the increased and decreased variability during cognitive decline and aging may be related to energy reallocation or different energy requirements among brain regions and across ages (Garrett

et al., 2011). This may provide a novel perspective to delineate cognitive and aging-related regional characteristics.

4.2 | Reallocation of energy distribution at multiple frequency bands during face recognition

Significant lfSSBR is evoked at the fundamental frequency and two harmonics along with power reduction at the 0.01–0.0475 Hz frequency band. The harmonic phenomenon is in line with previous steady-state evoked potential (SSEP) and lfSSBR studies (Chicherov & Herzog, 2015; Wang et al., 2014, 2016a), reflecting the dynamics of the nonlinear system (Herrmann, 2001; Lewis et al., 2016). The low-frequency power reduction is also observed in simple reaction task (He, 2011; Wang et al., 2014), working memory task (Fransson, 2006), and semantic comprehension task (Wang et al., 2015). It is suggested that, during cognitive processing, the brain reallocates energy from slow ongoing fluctuations to rapid cognition to improve behavioral performance and adaptation (He, Zempel, Snyder, & Raichle, 2010; Schroeder & Lakatos, 2012). However, the power reduction disappeared after the deconvolution of hemodynamic response function (Wang et al., 2014, 2015), indicating that neurovascular coupling may contribute to this phenomenon. The factors influencing neurovascular coupling, such as glucose metabolism and neurotransmitter reuptake reflected by cerebral blood flow and astrocyte activity, may contribute to the phenomenon of energy reallocation (Andreone, Lacoste, & Gu, 2015; Rosenegger & Gordon, 2015). This hypothesis deserves future investigations.

As the first study of frequency-specific BSV, we show that BSV has almost the same spatial distribution as power and is not always positively or negatively related to cognitive skill. In fact, the BSV is primarily increased at resonant frequencies while decreased at nonresonant frequencies, indicating frequency-specific energy reallocation. The frequency effect challenges the monotonous relationship between BSV and cognitive performance as previously suggested (Garrett et al., 2013a,2014), arguing that the brain can flexibly reallocate energy among different functional subsystems (Armbruster-Genç, Ueltzhöffer, & Fiebach, 2016).

4.3 | Brain–behavior relationship

Both power and variability have been demonstrated to be closely related to behavior performance (Garrett et al., 2014; Wang et al., 2015). In this study, the power and variability show consistent brain–behavior relationship. It could be found that cognitive-related energy reallocation occurs not only at resonant frequencies but also at nonresonant frequencies, indicating multifrequency or multitimescale energy reallocation. Additionally, the regions with strongest brain–behavior relationship did not significantly overlap with regions with strongest task effect, further supporting the nonmonotonic relationship between BSV and cognitive activity. Overall, these evidence extend the relatively clear BSV–behavior relationship to a flexible and nonmonotonic relationship.

Furthermore, whether power/variability increases or decreases may depend on parameters such as task, frequency, and brain region. Single-task and multitask may enable the brain to stay at a few stable states and transfer among multiple states, respectively, inducing distinctive power/variability changes. The task may induce complementary power/variability changes at task frequency and nontask frequency. High power/variability in the sensory cortex may be associated with more available sensory information, improving task performance (Lafontaine et al., 2016); whereas that in the task-control or decision-making regions may be related to multiple optional outputs, improving multitask performance but damaging single-task performance (Cole et al., 2013). In this study, higher power/variability in the visual system and attention system may be associated with more available input information and attention resources, respectively. These ample external and internal resources may result in better cognitive performance. By contrast, the frontal pole is involved in complex cognitive functions and behavioral control (Ray et al., 2015). Higher power/variability in this region may damage the output of single task. Therefore, we argue that a complex relationship between power/variability and behavioral performance may vary across space and time rather than a monotonous relationship for all spatiotemporal scales.

4.4 | Implications for future studies

We demonstrate that lfSSBR is closely related to brain signal variability, differentiating it from brain activation. The cognitive processes and ongoing activities are demonstrated to be negatively interactive and phase-dependent rather than linear addition (He, 2013; Huang et al., 2017), making the GLM-based brain activation inadequate to describe cognitive-related brain activity. By contrast, the lfSSBR could regulate phase synchronization at multiple frequency bands (Lewis et al., 2016; Wang et al., 2016a,b). The phase synchronization is essential to information transfer between brain regions (phase gating hypothesis) and to modulate high-frequency neural oscillations (phase-amplitude coupling hypothesis) (Canolty & Knight, 2010; Florin & Baillet, 2015; Maris, Fries, & van Ede, 2016). Furthermore, we suggest that lfSSBR is more powerful in predicting aging and behavioral performance than mean BOLD signal (Garrett et al., 2013a; Grady & Garrett, 2014; Guitart-Masip et al., 2016; McIntosh et al., 2008) due to the close relationship between power and variability. Overall, the lfSSBR may be a relative simple surrogate for nonlinear brain activity (e.g., harmonic phenomenon) with high SNR (>300% for lfSSBR as shown in Figure 2 vs 5% for mean BOLD signal change).

The consistent spatial distribution and brain–behavior relationship between power and variability is critical for us to understand the underlying mechanism of lfSSBR and the energy reallocation during face recognition. The high consistency of power/variability enables us to comprehend one from the other. For instance, we can explain lfSSBR from the opinion of complex system and describe variability from the perspective of frequency specificity. It is suggested that the brain, as a nonlinear dynamic system, acts at the "edge of criticality" among a variety of latent states or network configurations (Deco & Jirsa, 2012). Enhanced variability reflects greater network complexity, increased dynamic range, and the capacity for the system to explore different states (Garrett et al., 2011, 2013a). The energy reallocation associated with lfSSBR, therefore, is related to network reorganization and state transfer among frequency bands, in keeping with the multilayer network

hypothesis (Brookes et al., 2016; Wang et al., 2018). The reorganization of functional systems induced by face recognition across frequency bands and across brain regions is also in line with the idea of reorganization of functional networks and functional fingerprints during cognition (Ponce-Alvarez, He, Hagmann, & Deco, 2015; Siegel, Donner, & Engel, 2012). This may shed new insight into understanding how our brain mobilizes limited energy to optimize cognition (Raichle, 2006).

The current results could enlighten other neural oscillation researches such as SSEP and amplitude of low-frequency fluctuation (ALFF). We argue that the lfSSBR cannot be the mean response of multiple trials because the latter is associated with the mean rather than variance of brain signal. Likely, the SSEP may reflect the neural entrainment of task activities rather than the superposition of many event-related potentials (Zhang, Peng, Zhang, & Hu, 2013). On the other hand, we recommend researchers to explain the ALFF from the perspective of energy consumption and BSV, because the ALFF is the square root of power (Yang et al., 2007). Considering the extensive use of ALFF in cognitive and clinical neurosciences, we can understand the cognitive and pathologic mechanism of brain activities from the perspective of metastability, dynamic space, and kinetic energy revealed by BSV (Deco & Kringelbach, 2016; Garrett et al., 2014). In turn, the BSV may reflect the same neural and metabolic mechanisms as ALFF.

Furthermore, besides the fundamental frequency, the task effect on power and variability is located in different regions although the spatial distribution of these two indices is consistent. Considering that the brain signal is impossible to be precisely stable across trials (e.g., trial-to-trial variability), the moment-to-moment BSV may capture more details than the power of whole time series, making the task effects somewhat different between them. Alternatively, head motion and physiological contaminants may influence the spatial distributions of power and variability. However, we believe that these noises would exert comparable influences on power and variability as the close relationship between power and variability was revealed from both theoretical and empirical perspectives and the same noise processing method was used in the preprocessing section. The MSSD may be exquisitely sensitive to rapid head motion and physiological contaminants which are difficult to remove here. Rapid scanning techniques should be used in future studies to clarify the effect of these noises on power and variability.

Last, previous studies (Garrett et al., 2013b) and the current results suggest that power and variability are powerful indices in revealing brain responses to cognition, aging, and brain diseases at different temporal and spatial scales. However, more elaborate task design and noise control should be performed in future studies to make power and variability more powerful in predicting brain responses under various circumstances. Many indices such as power/variability, scale-free, and functional connectivity should be also combined to systematically uncover brain activities at multiple temporal and spatial scales.

5 | LIMITATIONS

Although the frequency-specific consistency of power and variability provides a promising insight regarding the multiscale neural oscillations, some limitations remain. First, due to the high accuracy of face recognition, we could not decipher the change of power–variability relationship and brain–behavior relationship associated with cognitive failure. As a consequence, the differences in these relationships between correct and incorrect trials could not be determined. Second, how does energy reallocation occur between different brain regions and frequency bands could not be determined here. Energy transfer between brain regions and frequency bands deserves future studies. Third, the high SNR of lfSSBR depends on regular task presentation in a relatively long time series (Norcia, Appelbaum, Ales, Cottereau, & Rossion, 2015), making it hard to be applied to event-related experimental design. Some other approaches with high SNR should be explored to capture brain activities in flexible task designs. Fourth, MSSD is sensitive to field strength differences in the BOLD signal across the brain. For instance, time series A: 1, 3, 5, 3, 1 has an MSSD of 1 while time series B: 1, 5, 9, 5, 1 has an MSSD of 4. However, they both have an MSSD value of ~1.43 if converting the time series to z-statistics before computing MSSD. The influences of normalization of time series on BSV and power have been demonstrated in previous studies (Garrett et al., 2011; Nomi et al., 2017) and in this study (Figure 2). Whether the normalization of time series would reflect different neural mechanisms compared with dataset without normalization requires a thorough examination by using both simulation and experimental data.

6 | CONCLUSIONS

In summary, we demonstrate that the power of brain signal is equivalent to the variability in the corresponding frequency band, arguing that the lfSSBR reflects the variance rather than the mean of brain signal. Therefore, this manuscript suggests that the lfSSBR reflects the entrainment mechanism rather than the mean response of multiple trials. Further, both power and variability analyses reveal complex energy reallocation pattern and brain–behavior relationship during face recognition, enlightening the multiscale adaptive energy reallocation of our brain during cognition.

ACKNOWLEDGMENT

All the authors have no conflict of interest to declare.

FUNDING

The work was supported by the 863 Project (2015AA020505), 111 Project (B12027), the Natural Science Foundation of China (61533006, 31600930, 31400901, and 61673089), the Science Foundation of Ministry of Education of China (14XJC190003), and the Fundamental Research Funds for the Central Universities (ZYGX2016KYQD120 and ZYGX2015J141).

ORCID

Bharat B. Biswal http://orcid.org/0000-0002-3710-3500
Huafu Chen http://orcid.org/0000-0002-4062-4753

REFERENCES

Andreone, B. J., Lacoste, B., & Gu, C. (2015). Neuronal and vascular interactions. *Annual Review of Neuroscience*, *38*, 25–46.

Armbruster-Genç, D. J. N., Ueltzhöffer, K., & Fiebach, C. J. (2016). Brain signal variability differentially affects cognitive flexibility and cognitive stability. *The Journal of Neuroscience*, *36*, 3978–3987.

Baldauf, D., & Desimone, R. (2014). Neural mechanisms of object-based attention. *Science (New York, N.Y.)*, *344*, 424–427.

Baria, A. T., Baliki, M. N., Parrish, T., & Apkarian, A. V. (2011). Anatomical and functional assemblies of brain BOLD oscillations. *The Journal of Neuroscience*, *31*, 7910–7919.

Bonini, F., Burle, B., Liégeois-Chauvel, C., Régis, J., Chauvel, P., & Vidal, F. (2014). Action monitoring and medial frontal cortex: Leading role of supplementary motor area. *Science*, *343*, 888–891.

Brookes, M. J., Tewarie, P. K., Hunt, B. A., Robson, S. E., Gascoyne, L. E., Liddle, E. B., … Morris, P. G. (2016). A multi-layer network approach to MEG connectivity analysis. *NeuroImage*, *132*, 425–438.

Canolty, R. T., & Knight, R. T. (2010). The functional role of cross-frequency coupling. *Trends in Cognitive Sciences*, *14*, 506–515.

Chicherov, V., & Herzog, M. H. (2015). Targets but not flankers are suppressed in crowding as revealed by EEG frequency tagging. *NeuroImage*, *119*, 325–331.

Cole, M. W., Reynolds, J. R., Power, J. D., Repovs, G., Anticevic, A., & Braver, T. S. (2013). Multi-task connectivity reveals flexible hubs for adaptive task control. *Nature Neuroscience*, *16*, 1348–1355.

Deco, G., & Jirsa, V. K. (2012). Ongoing cortical activity at rest: Criticality, multistability, and ghost attractors. *The Journal of Neuroscience*, *32*, 3366–3375.

Deco, G., & Kringelbach, M. L. (2016). Metastability and coherence: Extending the communication through coherence hypothesis using a whole-brain computational perspective. *Trends in Neurosciences*, *39*, 125–135.

Florin, E., & Baillet, S. (2015). The brain's resting-state activity is shaped by synchronized cross-frequency coupling of neural oscillations. *NeuroImage*, *111*, 26–35.

Fransson, P. (2006). How default is the default mode of brain function? Further evidence from intrinsic BOLD signal fluctuations. *Neuropsychologia*, *44*, 2836–2845.

Garrett, D. D., Kovacevic, N., McIntosh, A. R., & Grady, C. L. (2010). Blood oxygen level-dependent signal variability is more than just noise. *The Journal of Neuroscience*, *30*, 4914–4921.

Garrett, D. D., Kovacevic, N., McIntosh, A. R., & Grady, C. L. (2011). The importance of being variable. *The Journal of Neuroscience*, *31*, 4496–4503.

Garrett, D. D., Kovacevic, N., McIntosh, A. R., & Grady, C. L. (2013a). The modulation of BOLD variability between cognitive states varies by age and processing speed. *Cerebral Cortex*, *23*, 684–693.

Garrett, D. D., McIntosh, A. R., & Grady, C. L. (2014). Brain signal variability is parametrically modifiable. *Cerebral Cortex*, *24*, 2931–2940.

Garrett, D. D., Samanez-Larkin, G. R., MacDonald, S. W., Lindenberger, U., McIntosh, A. R., & Grady, C. L. (2013b). Moment-to-moment brain signal variability: A next frontier in human brain mapping? *Neuroscience & Biobehavioral Reviews*, *37*, 610–624.

Gonzalez-Castillo, J., Saad, Z. S., Handwerker, D. A., Inati, S. J., Brenowitz, N., & Bandettini, P. A. (2012). Whole-brain, time-locked activation with simple tasks revealed using massive averaging and model-free analysis. *Proceedings of the National Academy of Sciences*, *109*, 5487–5492.

Grady, C. L., & Garrett, D. D. (2014). Understanding variability in the BOLD signal and why it matters for aging. *Brain Imaging and Behavior*, *8*, 274–283.

Guitart-Masip, M., Salami, A., Garrett, D., Rieckmann, A., Lindenberger, U., & Bäckman, L. (2016). BOLD variability is related to dopaminergic neurotransmission and cognitive aging. *Cerebral Cortex*, *26*, 2074–2083.

Haxby, J. V., Hoffman, E. A., & Gobbini, M. I. (2000). The distributed human neural system for face perception. *Trends in Cognitive Sciences*, *4*, 223–233.

He, B. J. (2011). Scale-free properties of the functional magnetic resonance imaging signal during rest and task. *The Journal of Neuroscience*, *31*, 13786–13795.

He, B. J. (2013). Spontaneous and task-evoked brain activity negatively interact. *The Journal of Neuroscience*, *33*, 4672–4682.

He, B. J., Zempel, J. M., Snyder, A. Z., & Raichle, M. E. (2010). The temporal structures and functional significance of scale-free brain activity. *Neuron*, *66*, 353–369.

Herrmann, C. S. (2001). Human EEG responses to 1–100 Hz flicker: Resonance phenomena in visual cortex and their potential correlation to cognitive phenomena. *Experimental Brain Research*, *137*, 346–353.

Huang, Z., Zhang, J., Longtin, A., Dumont, G., Duncan, N. W., Pokorny, J., … Weng, X. (2017). Is there a nonadditive interaction between spontaneous and evoked activity? Phase-dependence and its relation to the temporal structure of scale-free brain activity. *Cerebral Cortex*, *27*, 1037–1059.

Lafontaine, M. P., Lacourse, K., Lina, J. M., Mcintosh, A. R., Gosselin, F., Théoret, H., & Lippé, S. (2016). Brain signal complexity rises with repetition suppression in visual learning. *Neuroscience*, *326*, 1–9.

Lewis, L. D., Setsompop, K., Rosen, B. R., & Polimeni, J. R. (2016). Fast fMRI can detect oscillatory neural activity in humans. *Proceedings of the National Academy of Sciences*,

Liang, X., Zou, Q., He, Y., & Yang, Y. (2013). Coupling of functional connectivity and regional cerebral blood flow reveals a physiological basis for network hubs of the human brain. *Proceedings of the National Academy of Sciences*, *110*, 1929–1934.

Maris, E., Fries, P., & van Ede, F. (2016). Diverse phase relations among neuronal rhythms and their potential function. *Trends in Neurosciences*, *39*, 86–99.

McDonnell, M. D., & Ward, L. M. (2011). The benefits of noise in neural systems: Bridging theory and experiment. *Nature Reviews Neuroscience*, *12*, 415–426.

McIntosh, A. R., Kovacevic, N., & Itier, R. J. (2008). Increased brain signal variability accompanies lower behavioral variability in development. *PLoS Computational Biology*, *4*, e1000106.

Mohr, P. N., & Nagel, I. E. (2010). Variability in brain activity as an individual difference measure in neuroscience? *The Journal of Neuroscience*, *30*, 7755–7757.

Nomi, J. S., Bolt, T. S., Ezie, C., Uddin, L. Q., & Heller, A. S. (2017). Moment-to-moment BOLD signal variability reflects regional changes in neural flexibility across the lifespan. *The Journal of Neuroscience*, *37*, 5539–5548.

Norcia, A. M., Appelbaum, L. G., Ales, J. M., Cottereau, B. R., & Rossion, B. (2015). The steady-state visual evoked potential in vision research: A review. *Journal of Vision*, *15*, 1–46.

Ponce-Alvarez, A., He, B. J., Hagmann, P., & Deco, G. (2015). Task-driven activity reduces the cortical activity space of the brain: Experiment and whole-brain modeling. *PLoS Computational Biology*, *11*, e1004445.

Raichle, M. E. (2006). The brain's dark energy. *Science (New York, N.Y.)*, *314*, 1249–1250.

Raichle, M. E. (2015). The brain's default mode network. *Annual Review of Neuroscience*, *38*, 433–447.

Ray, K. L., Zald, D. H., Bludau, S., Riedel, M. C., Bzdok, D., Yanes, J., … Eickhoff, S. B. (2015). Co-activation based parcellation of the human frontal pole. *NeuroImage*, *123*, 200–211.

Rosenegger, D. G., & Gordon, G. R. (2015). A slow or modulatory role of astrocytes in neurovascular coupling. *Microcirculation (New York, N.Y. : 1994)*, *22*, 197–203.

Rossion, B., Prieto, E. A., Boremanse, A., Kuefner, D., & Van Belle, G. (2012). A steady-state visual evoked potential approach to individual face perception: Effect of inversion, contrast-reversal and temporal dynamics. *NeuroImage*, *63*, 1585–1600.

Samanez-Larkin, G. R., Kuhnen, C. M., Yoo, D. J., & Knutson, B. (2010). Variability in nucleus accumbens activity mediates age-related suboptimal financial risk taking. *The Journal of Neuroscience*, *30*, 1426–1434.

Schroeder, C. E., & Lakatos, P. (2012). The signs of silence. *Neuron*, *74*, 770–772.

Siegel, M., Donner, T. H., & Engel, A. K. (2012). Spectral fingerprints of large-scale neuronal interactions. *Nature Reviews Neuroscience*, *13*, 121–134.

Sokunbi, M. O. (2014). Sample entropy reveals high discriminative power between young and elderly adults in short fMRI data sets. *Frontiers in Neuroinformatics*, *8*, 69.

Wang, Y.-F., Dai, G.-S., Liu, F., Long, Z.-L., Yan, J. H., & Chen, H.-F. (2015). Steady-state BOLD response to higher-order cognition modulates low frequency neural oscillations. *Journal of Cognitive Neuroscience*, *27*, 2406–2415.

Wang, Y.-F., Liu, F., Long, Z.-L., Duan, X.-J., Cui, Q., Yan, J. H., & Chen, H.-F. (2014). Steady-state BOLD response modulates low frequency neural oscillations. *Scientific Reports*, *4*, 7376.

Wang, Y., Liu, F., Jing, X., Long, Z., & Chen, H. (2016a). Phase-dependent alteration of functional connectivity density during face recognition in the infra-slow frequency range. In R. Wang & X. Pan (Eds.), *Advances in cognitive neurodynamics (V)* (pp. 305–310). Singapore: Springer Singapore.

Wang, Y., Liu, F., Li, R., Yang, Y., Liu, T., & Chen, H. (2013). Two-stage processing in automatic detection of emotional intensity: A scalp event-related potential study. *Neuroreport*, *24*, 818–821.

Wang, Y., Zhu, L., Zou, Q., Cui, Q., Liao, W., Duan, X., … Chen, H. (2018). Frequency dependent hub role of the dorsal and ventral right anterior insula. *NeuroImage*, *165*, 112–117.

Wang, Y. F., Long, Z., Cui, Q., Liu, F., Jing, X. J., Chen, H., … Chen, H. F. (2016b). Low frequency steady-state brain responses modulate large scale functional networks in a frequency-specific means. *Human Brain Mapping*, *37*, 381–394.

Worsley, K. J., Marrett, S., Neelin, P., Vandal, A. C., Friston, K. J., & Evans, A. C. (1996). A unified statistical approach for determining significant signals in images of cerebral activation. *Human Brain Mapping*, *4*, 58–73.

Yan, C.-G., & Zang, Y.-F. (2010). DPARSF: A MATLAB toolbox for "pipeline" data analysis of resting-state fMRI. *Frontiers in Systems Neuroscience*, *4*, 1–7.

Yang, H., Long, X.-Y., Yang, Y., Yan, H., Zhu, C.-Z., Zhou, X.-P., … Gong, Q.-Y. (2007). Amplitude of low frequency fluctuation within visual areas revealed by resting-state functional MRI. *NeuroImage*, *36*, 144–152.

Zhang, L., Peng, W., Zhang, Z., & Hu, L. (2013). Distinct features of auditory steady-state responses as compared to transient event-related potentials. *PLoS ONE*, *8*, e69164.

Zuo, X.-N., Di Martino, A., Kelly, C., Shehzad, Z. E., Gee, D. G., Klein, D. F., … Milham, M. P. (2010). The oscillating brain: Complex and reliable. *NeuroImage*, *49*, 1432–1445.

How to cite this article: Wang Y, Chen W, Ye L, et al. Multiscale energy reallocation during low-frequency steady-state brain response. *Hum Brain Mapp*. 2018;39:2121–2132. https://doi.org/10.1002/hbm.23992